**Biotechnology**
Journal

RESEARCH ARTICLE

# Cascade reactions with two non-physiological partners for NAD(P)H regeneration via renewable hydrogen

**Francisco Gasteazoro**[1,2] | **Gianluca Catucci**[1] | **Lisa Barbieri**[1,3] | **Melissa De Angelis**[1] | **Alessandro Dalla Costa**[1] | **Sheila J. Sadeghi**[1] | **Gianfranco Gilardi**[1] | **Francesca Valetti**[1]

[1]Department of Life Sciences and Systems Biology, University of Torino, Torino, Italy

[2]CICATA Unidad Morelos, Instituto Politécnico Nacional, Mexico D. F., Mexico

[3]University School for Advanced Studies IUSS Pavia, Pavia, Italy

**Correspondence**
Francesca Valetti, Department of Life Sciences and Systems Biology, University of Torino, Torino, Italy.
Email: francesca.valetti@unito.it

## Abstract

An attractive application of hydrogenases, combined with the availability of cheap and renewable hydrogen (i.e., from solar and wind powered electrolysis or from recycled wastes), is the production of high-value electron-rich intermediates such as reduced nicotinamide adenine dinucleotides.

Here, the capability of a very robust and oxygen-resilient [FeFe]-hydrogenase (CbA5H) from *Clostridium beijerinckii* SM10, previously identified in our group, combined with a reductase (BMR) from *Bacillus megaterium* (now reclassified as *Priestia megaterium*) was tested. The system shows a good stability and it was demonstrated to reach up to $28 \pm 2$ nmol NADPH regenerated s$^{-1}$ mg of hydrogenase$^{-1}$ (i.e., $1.68 \pm 0.12$ U mg$^{-1}$, TOF: $126 \pm 9$ min$^{-1}$) and $0.46 \pm 0.04$ nmol NADH regenerated s$^{-1}$ mg of hydrogenase$^{-1}$ (i.e., $0.028 \pm 0.002$ U mg$^{-1}$, TOF: $2.1 \pm 0.2$ min$^{-1}$), meaning up to 74 mg of NADPH and 1.23 mg of NADH produced per hour by a system involving 1 mg of CbA5H. The TOF is comparable with similar systems based on hydrogen as regenerating molecule for NADPH, but the system is first of its kind as for the [FeFe]-hydrogenase and the non-physiological partners used. As a proof of concept a cascade reaction involving CbA5H, BMR and a mutant BVMO from *Acinetobacter radioresistens* able to oxidize indole is presented. The data show how the cascade can be exploited for indigo production and multiple reaction cycles can be sustained using the regenerated NADPH.

**KEYWORDS**
bio-catalysis, cofactor recycling, hydrogenase, metalloenzyme , NADH, NADPH, oxygen-resilience, P450 BM3

## 1 | INTRODUCTION

Biocatalysis is becoming increasingly important in the field of industrial biotechnologies.[1–3] For industrial application, reactions catalyzed by

NAD(P)H dependent oxidoreductases are extremely relevant for the production of enantiomeric compounds. Given the high cost, stoichiometric usage, and physical instability of NAD(P)H, a suitable method for regeneration is essential for practical application.[4]

The enzymatic approach is usually associated with high specific activity and low energy consumption.[4] Moreover, it has a

Francisco Gasteazoro and Gianluca Catucci contributed equally.

relatively higher total turnover numbers (TTNs) compared to chemical or electrochemical methods.[5]

So far, the enzymatic methods proposed for NAD(P)H regeneration relies mainly on glucose dehydrogenase for NADPH recycling as demonstrated in the biosynthesis of ethyl (S)-4-chloro-3-hydroxybutyrate, a key intermediate in the production of atorvastatin,[6] while formate dehydrogenase can provide a valuable NADH recycling method, by converting formate to $CO_2$. An example of application of the latter is the industrial production by Evonik-Degussa of enantiopure S-*tert*-leucine starting from trimethylpyruvate[7–10] as valuable intermediate in the synthesis of inhibitors of the hepatitis C virus NS3 protease[11] or for the production of better tolerated immunosuppressants.[12] Both methods, although displaying fairly high turnover frequencies[13,14] suffer from drawbacks due to the accumulating by-products, $\beta$-D-glucono-1,5-lactone for glucose dehydrogenase and $CO_2$ for formate dehydrogenase, leading to a general acidification in aqueous solution[4] and, in the first case, also to the requirement for expensive and time-consuming purification of the main enzymatic reaction product of interest for which the cofactor regeneration is ancillary. Other methods have been proposed based on ADH (including hybrid systems with $TiO_2$-nanoreactors)[15] or phosphite dehydrogenase,[16,17] but the systems are less efficient and do not provide solution to accumulation of by-products or pH instability. Whole-cell approaches were also proposed, based on TCA cycle enzymes and citrate, but this would introduce even further complexity to the reaction system.[18]

Alternatively, the use of gaseous hydrogen as a source of reduction equivalents allows efficient recycling of NAD(P)H without the formation of by-products that could alter the pH or complicate product recovery. Also, the availability of cheap hydrogen from renewable energy sources such as solar and wind powered electrolysis or as bio-hydrogen from dark fermentation of organic fraction of municipal solid wastes, green and agri-food wastes[19,20] can ensure the sustainability of the process and be in line with a circular economy paradigm. Although the production of green hydrogen is still not optimized and the cost is not matching yet market requirements,[21] low-cost methods are being implemented and quickly developing, the estimated $H_2$ cost is 2.57$ $kg^{-1}$ $H_2$ for dark fermentation and 2.83$ $kg^{-1}$ $H_2$ for photofermentation.[22]

The intriguing possibility of using hydrogen as regenerating co-substrate for the high value NADPH is here explored via an enzyme belonging to a different class from the already proposed soluble $NAD(P)^+$-dependent [NiFe]-hydrogenases from *Pyrococcus furiosus* (PfSH)[23–25] and from *Cupriavidus necator* (ReSH),[26,27] that of [FeFe]-hydrogenases, generally more processive than [NiFe]-hydrogenase, but more oxygen sensitive.[28,29] CbA5H from *Clostridium beijerinckii* SM10 represents an exception, given its unusual oxygen-resilience.[30–33] The resilience does not imply tolerance, and CbA5H is inactive in presence of oxygen, but it can be quickly and repeatedly reactivated by hydrogen flushing with little loss of activity,[32] allowing for alternative cycling of hydrogen or oxygen if this latter is required in the NADPH consuming half of the reaction. A very recent paper also suggests an improved recovery by increased enzyme flexibility.[34] This robust [FeFe]-hydrogenase is here tested in combination with non-

physiological partners, already used in modular "Lego approach" for protein engineering.[35–40] These are reductases of P450 cytochromes, namely BMR from *Bacillus megaterium*,[41,42] now reclassified as *Priestia megaterium*, and human CPR.[43] As separated proteins or as domains (resulting from gene fusion), these reductases provide the electrons to the P450 heme-containing active site, required to reductively cleave $O_2$, releasing an oxygenated organic product and a molecule of water as in the following general reaction,

$$R + 2\,H^+ + 2\,e^- + O_2 \rightarrow ROH + H_2O.$$

which may also lead to less usual reactions such as demethylation, deformylation, epoxidation, rearrangements, and coupling.[44–46]

The two required electrons are accepted by the reductase from NAD(P)H as an $H^-$ ion and, via an FAD domain and an FMN domain, transferred, one electron at a time, to the cytochromes P450 heme.[47]

Here the reverse reaction (i.e., of electrons delivery to the $NAD(P)^+$) is exploited, demonstrating an intriguing role of one of the two tested reductases, with the NAD(P)H binding domain representing an "adapting plug-in" for the regeneration of the pyridinic cofactor coupled to the hydrogenase activity via the FAD and FMN cofactors of the reductase.

## 2 | MATERIALS AND METHODS

### 2.1 | Materials

All the media and chemicals were analytical grade, purchased from Merck (Darmstadt, Germany) and Carlo Erba Reagents (Milan, Italy). Desthiobiotin, StrepTag resin, and HABA for the CbA5H purification were purchased from IBA Lifesciences GmbH (Göttingen, Germany).

### 2.2 | Protein expression and purification

CbA5H was expressed as reported,[32] with minor changes. Briefly, plasmid pECbA5H, containing the CbA5H encoding gene *Cb1773*[32] and the maturase gene *hydE* from *Clostridium acetobutylicum*,[48] was transformed into *Escherichia coli* BL21/pFG (containing the plasmid pCaFG, with the maturase genes *hydF* and *hyd G* from *C. acetobutylicum*).[48] Plates with streptomycin and ampicillin were used to grow the cells.

For the expression, a single colony was used to inoculate 20 mL culture incubated O.N. (LB + amp + str 37°C, 200 rpm). The next day, the preculture was used to inoculate 1 L of culture (2 L total flask volume). Each flask contained: 900 mL TB, 100 mL potassium phosphate solution (2.2 g $KH_2PO_4$, 9.4 g $K_2HPO_4$), 2 mM ferric ammonium citrate, 100 μg $mL^{-1}$ ampicillin, and 50 μg $mL^{-1}$ streptomycin. The cultures were incubated at 37°C, 200 rpm util $OD_{600} = 0.4–0.6$, then supplemented with 0.5% glucose, 25 mM sodium fumarate, 2 mM cysteine, and 1.5 mM IPTG. The cultures were transferred in 2 L bottles and kept under anaerobic conditions flushing argon for 24 h at 20°C.[49] Differently from[32] the cultures were centrifuged in aerobic condition (without observing activity loss in the further steps) and the pellet was stored at −20°C until further use.

CbA5H purification was performed in aerobic condition, exploiting the inactivated stable form of the protein, using Strep-Tactin Superflow high-capacity resin (IBA), following the manufacturer's protocol. The enzyme was eluted with 5 mM desthiobiotin in buffer W (100 mM TrisHCl, 150 mM NaCl, pH 8.0), checked for purity via SDS-PAGE, concentrated, and stored with buffer W.

For BMR production, the pCW-Ori(+)-BMR vector[35] was transformed into *E. coli* DH5$\alpha$ cells. Expression and purification was performed as described.[35] The purest fractions were pooled and stored in storage buffer (KPi 100 mM pH 7.6, 10% glycerol) at −80°C for further use.

Human CPR was expressed as a full-length protein in *E. coli* DH5$\alpha$ as previously described.[50] CPR concentrations were measured using an extinction coefficient at 456 nm of 24,100 $M^{-1}$ $cm^{-1}$.[51]

## 2.3 | NAD(P)H regeneration activity assays

Enzymatic cofactor regeneration was tested using an Agilent UV-Vis spectrophotometer (845x system) by measuring the increase of absorbance at 340 nm due to the accumulated NAD(P)H.

One milliliter Quartz cuvettes were used to carry out the tests, which were typically performed using CbA5H and either BMR or CPR on 1 mM $NADP^+$ or 1 mM $NAD^+$. Optimal reactions contained: BMR 0.23 µM, CbA5H 0.23 µM in buffer W (TrisHCl 100 mM, NaCl 150 mM; pH 8.0).

In general, two cuvettes were prepared, one control containing only buffer W, $NADP^+/NAD^+$ and one also containing reductase (BMR/CPR). Both cuvettes (without CbA5H hydrogenase), closed with a silicone stopper, were placed under $H_2$ flow for 10–15 min each and then placed on ice. The CbA5H was placed in a small, sealed bottle and reactivated sparging $H_2$ into the solution for 10 min. It was then placed on ice for 30 min before being added to the cuvettes to start the reaction.

The spectrophotometer Peltier system was set at a temperature of 37°C; kinetics of reaction (monitored with wavelength setup at 340 nm) was performed with different runtimes (180–1200 s).

The experiment was set up blanking with the control cuvette without the hydrogenase; afterwards, hydrogenase was added to the cuvettes with a syringe without removing the silicone caps. The control cuvette without the reductase (BMR/CPR) was tested with the same setup and runtime of the counterpart containing BMR or CPR to exclude any unspecific reduction of the cofactors. Also, this cuvette was used to check the uptake activity of the hydrogenase alone when compared with negative results on the experimental cuvette, by adding methyl viologen to a final concentration of 10 mM. Reduction of methyl viologen was followed measuring the increase of absorbance at 604 nm, using a molar extinction coefficient of 13.6 $mM^{-1}$ $cm^{-1}$. The recorded CbA5H uptake activity in all validated tests in buffer W were within the expected range of 150–200 µmol $H_2$ $min^{-1}$ $mg^{-1}$.[30,32]

For the activity test at different KCl concentration and at different [CbA5h] to [BMR] ratio, buffer W was replaced with 50 mM TrisHCl buffer pH 8.0. All other parameters were kept the same.

The NAD(P)H regeneration specific activity is expressed as U $mg^{-1}$ of hydrogenase, where U are µmol NAD(P)H regenerated $min^{-1}$ as usually reported in literature.[24,52,53]

## 2.4 | Differential scanning calorimetry (DSC) measurement

DSC was carried out on a Microcal VP-DSC instrument from Malvern Panalytical Ltd (Malvern, UK) with the following set-up: 25–90°C temperature gradient, 90°C $h^{-1}$ scan rate, and 10 min pre-scan equilibration.[54,55] A solution at a final concentration of 8 µM of each enzyme (previously undergone to thoroughly exchanges with argon saturated buffer W) was incubated in argon saturated buffer W (100 mM TrisHCl, 150 mM NaCl) for the single CbA5H and BMR scan. The same final concentration of 8 µM per each protein and the same in argon saturated buffer W batch was used in the combined BMR and CbA5H. Data analysis was performed using Microcal Origin software (Malvern). Cycles of cooling and reheating of the samples were performed to obtain the background for buffer subtraction or test hypothetical refolding. Replicate runs did not vary more than 0.25°C. None of the proteins exhibited even partial re-folding upon cooling and re-heating the sample indicating full irreversibility of the unfolding processes.

## 2.5 | Isothermal titration calorimetry

Isothermal titration calorimetry (ITC) experiments were performed at 25°C using a MicroCal iTC200 instrument (Malvern Instruments, Malvern). Before the experiment, CbA5H and BMR were prepared by extensive buffer-exchange using Amicon centrifugal filters (30 kDa MWCO) and concentrated with the same buffer (trial were performed either with buffer W pH 8.0 or with 100 mM KPi, 10% glycerol, pH 7.0, the second resulting in a better BMR stabilization in the assay conditions). The reaction cell was filled with 300 µL of 80 µM CbA5H and the injection syringe was filled with 1200 µM BMR. BMR was titrated into CbA5H up to a 1:3 (CbA5H:BMR) molar ratio.

The first injection was 0.1 µL with 0.2 s duration and omitted during data analysis. The other injections were 3.6 µL with 4 s duration. Each titration experiment involved a 180 s interval between injections. The reaction cell was continuously stirred at 750 rpm speed. A reference power of 10 µcal $s^{-1}$ was used for each experiment. The data were processed and analyzed by using Origin 7.0 software.

## 2.6 | Assay of BVMO R292A mutant biocatalysis with CbA5H/BMR NADPH regeneration system

BVMO R292A mutant was expressed and purified as previously described.[56,57] The assay for indigo production was performed by monitoring the increase in absorbance at 620 nm in presence of the NADPH regenerating system and NADPH consumption rates (AU $s^{-1}$)

at 340 nm, using an Agilent UV-Vis spectrophotometer (845x system). This first step was performed in aerobic conditions in a total volume of 1 mL containing 2 µM BVMO R292A mutant, 5 mM indole, 0.23 µM BMR, 0.23 µM CbA5H in buffer W (TrisHCl 100 mM, NaCl 150 mM; pH 8.0) and approximately 145 µM of NADPH (Abs$_{340nm}$ = 0.9, $\varepsilon$ = 6220 M$^{-1}$ cm$^{-1}$) regenerated from 1 mM NADP$^+$ in a typical reaction as described in Section 2.3. Reactions were followed for 1800 s (time required to completely consume NADPH) at 25°C, in order to maintain the BVMO more stable.[57] The reaction was then centrifuged at 12,000 × $g$ for 10 min and the pellet containing the produced indigo was resuspended in 1 mL of DMSO and the spectrum was recorded. The supernatant was flushed with pure hydrogen for 10 min on ice in a sealed 1 mL cuvette to regenerate NADPH. The reaction was followed at 340 nm to check NADPH regeneration completeness by recording the kinetics after blanking with the flushed mixture and recording the spectra for the following 3600 s until it reached a plateau. The regenerated NADPH was then used in a further step simply exposing the mixture to air, thus allowing the oxygen co-substrate to access the mixture for the BVMO R292A mutant reaction, which was followed at 620 nm to monitor indigo production at 25°C for 2000 s. The reaction was centrifuged at 12,000 × $g$ for 10 min again to harvest the produced indigo which was resuspended in 1 mL DMSO and whose spectrum was recorded as previously mentioned.

# 3 | RESULTS

## 3.1 | Activity test of the redox partners

CbA5H [FeFe]-hydrogenase was tested with BMR and CPR reductases.

A general overview of the structure and surface features of the involved redox partners is reported in Figure 1.

The activity of NAD(P)H production was only observed in the system with the combination of CbA5H and BMR, while CPR did not sustain the pyridinic cofactor regeneration (Figure 2). No activity was observed using either of the redox partner alone or by saturating the cuvette solution and headspace with nitrogen or argon. The uptake activity of the CbA5H alone in each experimental session was confirmed to be within the range of 150–200 µmol H$_2$ min$^{-1}$ mg$^{-1}$ as expected in buffer W.[30,32]

The system was optimized as for buffer type and pH ensuring the highest hydrogenase stability with buffer W, which was confirmed to be the best option, and testing the stoichiometric ratio of CbA5H to BMR (testing a range of concentration of 0.06–0.57 µM of BMR and 0.2–0.66 µM of CbA5H monomer, and a range of CbA5H monomer to BMR ratio of 1:1.6–1:0.18) which was observed to be a 1:1 ratio of the CbA5H monomer to the BMR, both in buffer W and in 50 mM TrisHCl pH 8.0 (Figure 3B).

An example of a typical kinetic of NADPH regeneration is reported in Figure 2A. The increase in absorbance at 340 nm was used to calculate the reaction rate, using an extinction coefficient of 6220 M$^{-1}$ cm$^{-1}$. The system reached up to 28 ± 2 nmol NADPH regenerated s$^{-1}$ mg of hydrogenase$^{-1}$ (i.e., 1.68 ± 0.12 U mg$^{-1}$, TOF: 126 ± 9 min$^{-1}$) meaning up to 74 mg of NADPH produced per hour by a system involving 1 mg of CbA5H.

The same approach applied to the regeneration of NADH yielded a lower amount, as it can be appreciated in Figure 2B. The calculation returned a value of 0.46 ± 0.04 nmol NADH regenerated s$^{-1}$ mg of hydrogenase$^{-1}$ (i.e., 0.028 ± 0.002 U mg$^{-1}$, TOF: 2.1 ± 0.2 min$^{-1}$) meaning 1.23 mg of NADH produced per hour by a system involving 1 mg of CbA5H.

## 3.2 | CbA5H/BMR interaction dependence upon changing salt concentration and ratio

A test on the dependence of activity upon varying salt concentration was performed in order to obtain further information on the recognition pattern and chemical stabilization involved in the redox partners interaction. In this case buffer W was replaced with a lower ionic strength 50 mM TrisHCl buffer pH 8.0 to avoid shielding effect in charge–charge interaction due to the buffer. KCl was used at different concentration ranging from 30 to 130 mM. All the other settings and protein concentration were kept as in the standard activity assay. The obtained data are reported in Figure 3A. A larger variability of the measurements was observed in this case, as reported in the error bars of the graph, possibly due to a lower stabilizing effect of the chosen buffer to the hydrogenase CbA5H (for which buffer W is the ideal system). No significative difference of activity can be claimed upon increasing salt concentration in this experimental set-up.

The same low ionic strength buffer (50 mM TrisHCl pH 8.0, without added KCl) was also used to confirm the optimal 1:1 CbA5H (monomer) to BMR stoichiometric ratio which was firstly observed and applied in buffer W. Figure 3B reports the obtained results. A significatively lower NADPH regeneration activity is observed upon slightly decreasing or increasing the 1:1 optimal ratio. The same trend was observed in buffer W, with a drop of activity up to 5% of the optimal activity upon reaching a value of 1:2 of the CbA5H (monomer) to BMR stoichiometric ratio (data not shown).

## 3.3 | DSC and ITC analysis

In order to further explore the reciprocal interaction between CbA5H and BMR, enabling the recorded activity on NADPH and NADH regeneration, DSC and ITC tests were run. The DSC allows to measure the stability of the isolated protein and reciprocal stabilization or destabilization effects of each protein to the other.

The observed traces (Figure 4) of the single proteins confirmed the previously observed stability features of the isolated BMR (in blue) and [FeFe]-hydrogenase (in black). The trace in red shows the experimental result of the solution with the combined proteins in the 1:1 stoichiometric ratio (demonstrated as optimal in the activity test). The overlapping of the maximal values of the peaks in the single protein and combined proteins experiments indicate that no major destabilization effect is generated by the interaction of the two proteins.
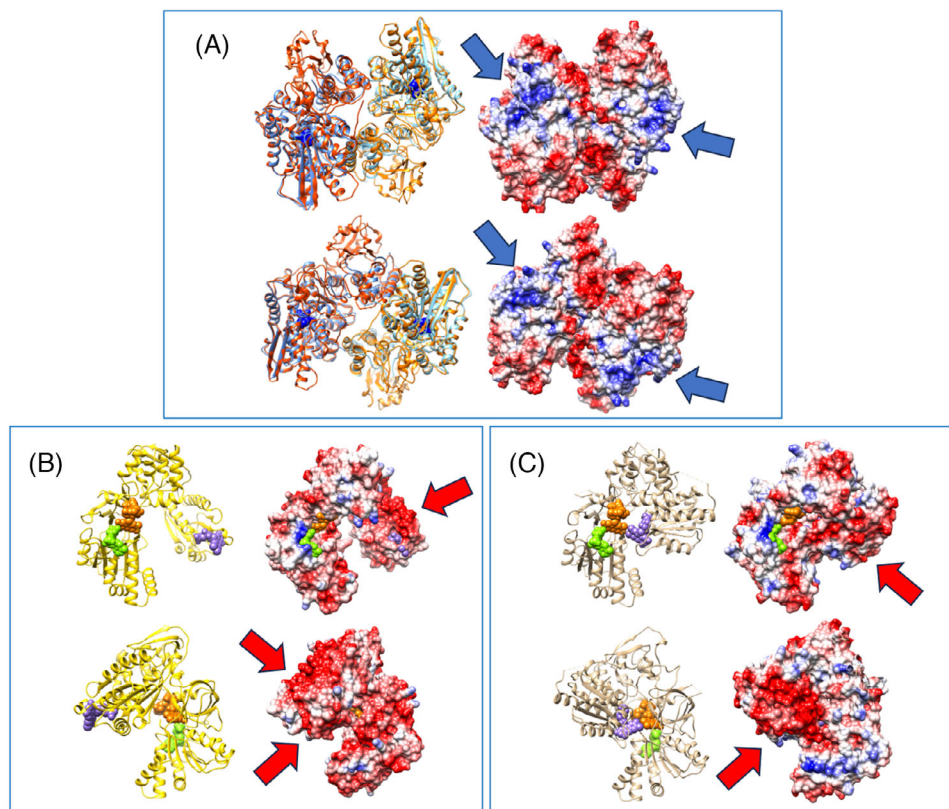
**FIGURE 1** Overview of the structure and surface potential features of the considered redox proteins. (A) Structure of CbA5H, based on the PDB 6TTL in blue/light blue and overlapped model (AF-A0A1I9RYV3-F1-model_v4.pdb) obtained with AlphaFold2 in orange/light orange (the model also contains the FeS domain not resolved in 6TTL). The H-cluster in the active site is represented in blue and space fill. The crystallographic functional dimer is reported in the picture (lighter and darker colors for each subunit). The surface was calculated with chimera and colored according to Coulombic potential scale of $-10$ to $+10$ kcal $(mol \cdot e)^{-1}$ at 298 K, a dielectric constant of 4.0 and a default distance from surface of 1.4 Å, to evaluate the potential of the solvent-accessible surface. Two poses (corresponding orientation of ribbon and surface representation) are reported (top and bottom). Blue arrows indicate the positive patches putatively involved in the interaction with negative surfaces of ferredoxin (physiological) or BMR/CPR (non-physiological). (B) BMR structure and corresponding surface Coulombic potential (as described for A). The BMR is represented in the open conformation, checked for consistency with PDB: 4DQL for reductase crystal structure of the FAD binding domain of cytochrome P450 BM3 in complex with NADP$^+$ but represented here by the whole BMR model obtained with AlphaFold2 AF-P14779-F1-model_v4.pdb (including the FMN domain which is missing in the crystal structure), using the aminoacidic same sequence of the real protein expressed for the experiments (aa 477–1054 of the P450 BM3 full protein). The NADP$^+$ and FAD cofactors were represented by structural overlapping with the PDB: 4DQL, while the FMN cofactor was represented by overlapping with the crystal structure of *Desulfovibrio vulgaris* flavodoxin (PDB: 1XT6, NADP$^+$ is represented in green, FAD in orange and FMN in purple). Red arrows indicate possible negative patches to drive interaction for the non-physiological complex with CbA5H. (C) CPR structure (wild type human CYPOR closed conformation), crystal structure PDB: 5FA6 and corresponding surface Coulombic potential (as described for A). NADP$^+$ is represented in green, FAD in orange and FMN in purple. Red arrows indicate possible negative patches to drive interaction for the non-physiological complex with CbA5H.

In order to measure the possible formation of a stable CbA5H–BMR complex different ITC experiments were carried out (Figure S1A–C) where both protein concentrations and molar ratio were changed. Most of the experiment did not clearly lead to the formation of a molecular complex, but in one case when CbA5H and BMR concentrations were used at 80 and 1200 μM (Figure S1C) an endergonic interaction between the two redox partners was detected. Nevertheless, the signal was very low compared to the baseline (Figure S1C); therefore, the interaction could not be translated into a binding affinity. Indeed, further increase of the two enzymes concentration would lead to protein precipitation/aggregation.

## 3.4 | Biocatalysis application

A real application to biocatalysis was performed using a mutant of a Baeyer-Villiger monooxygenase from *Acinetobacter radioresistens* S13 (Ar-BVMO R292A). This mutant can efficiently perform the NADPH and oxygen dependent hydroxylation of indole on C2 or C3, granting two oxidized products which in turn can non-enzymatically generate indigo or indirubin.[57] The NADPH generated by the CbA5H/BMR system in a typical experiment as reported in Figure 2A was used to drive the BVMO reaction as shown in Figure 5A STEP 1. The absorbance spectra recorded during the reaction show a decrease at 340 nm,
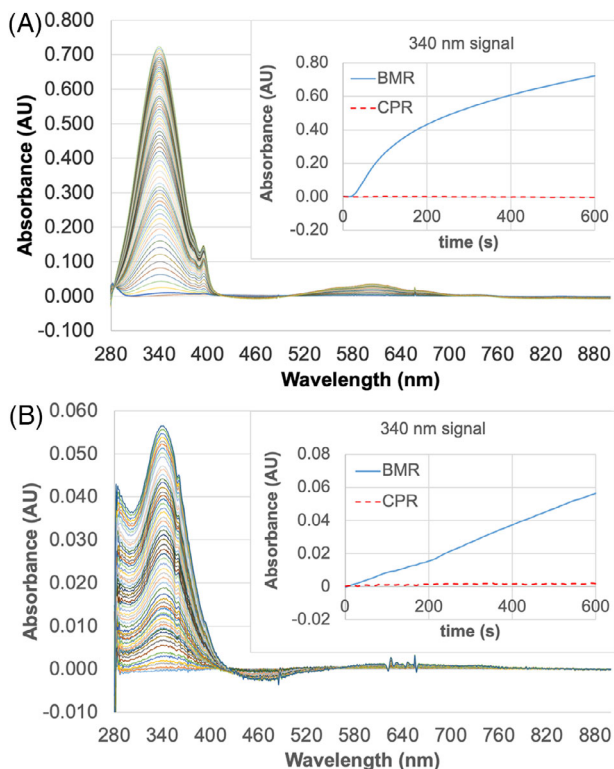
**FIGURE 2** (A) Regeneration of NADPH, typical trace, 1 mM NADP$^+$, BMR 0.23 μM, CbA5H 0.23 μM in buffer W (TrisHCl 100 mM, NaCl 150 mM; pH 8.0), 37°C. (B) Regeneration of NADH, typical trace, 1 mM NAD$^+$, BMR 0.23 μM, CbA5H 0.23 μM in buffer W (TrisHCl 100 mM, NaCl 150 mM; pH 8.0), 37°C. For both (A) and (B) experiment details as in Section 2. The rates are calculated as initial rates in the linear part of the kinetics avoiding (when needed) the short initial lag. The reported spectra (sampled each 10 s) indicate the increasing 340 nm peak associated to NAD(P)H accumulation. Kinetic traces are reported compared to the negative experiments with CPR 0.23 μM replacing BMR and keeping the same conditions.



**FIGURE 3** (A) Dependence of the reaction rates of NADPH reduction by hydrogen, in the system CbA5H-BMR in 50 mM TrisHCl, pH 8.0, on different concentration of KCl. Reactions were performed at 37°C (BMR 0.23 μM, CbA5H 0.23 μM, NADP$^+$ 1 mM). Error bars indicate the SD on triplicate independent experiments. Statistical relevance of the differences detected between the collected results was analyzed by one-way analysis of variance (ANOVA) followed by Tukey–Kramer post-hoc test. $p$ values were always >0.05 (ranging between 0.809 and 1), indicating there is no significant difference between the means of any pair upon changing KCl concentration. The 100% activity here is $7.2 \pm 0.73$ nmol NADPH regenerated s$^{-1}$ mg of hydrogenase$^{-1}$. Activity in 50 mM TrisHCl, pH 8.0 is approximately 25% of the activity recorded in the optimal buffer W. (B) Dependence of the reaction rates of NADPH reduction by hydrogen, in the system CbA5H-BMR in 50 mM TrisHCl, pH 8.0, on different CbA5H (monomer) to BMR stoichiometric ratios and with different absolute amounts of proteins. Activity was always normalized by referring to hydrogenase amount: 100% activity here is $6.9 \pm 0.35$ nmol NADPH regenerated s$^{-1}$ mg of hydrogenase$^{-1}$. Reactions were performed at 37°C (BMR in the range 0.063–0.571 μM, CbA5H in the range 0.328–0.656 μM, NADP$^+$ 1 mM). Error bars indicate the SD on triplicate independent experiments. Significance differences, compared to 1:1 ratio, are indicated as evaluated by one-way ANOVA followed by Tukey–Kramer post-hoc test. $^*p < 0.01$, $^\#p < 0.001$.

indicating the NADPH consumption, and a specific increase at 620 nm related to the indigo production.

The reaction was performed for 30 min at 25°C (temperature was selected to ensure maximum stability of Ar-BVMO R292A) to consume all NADPH and the indigo produced was then centrifuged and resuspended in DMSO (Figure 5B, left spectrum). In STEP 2 (Figure 5A) the supernatant of STEP 1, containing Ar-BVMO R292A, BMR, and CbA5H, was flushed with hydrogen allowing the regeneration of NADPH as indicated in the corresponding trace at 340 nm (Figure 5A STEP 2) absorbance at 340 nm increased (indicating NADPH regeneration, spectra reported in Figure S4) and reached a plateau after 3600 s and the cuvette was exposed to oxygen again in STEP 3, so that the NADPH formed in STEP 2 could sustain a further production of indigo as indicated in the 620 nm trace of STEP 3 and in the spectrum of the precipitated and resuspended indigo of Figure 5B (right).
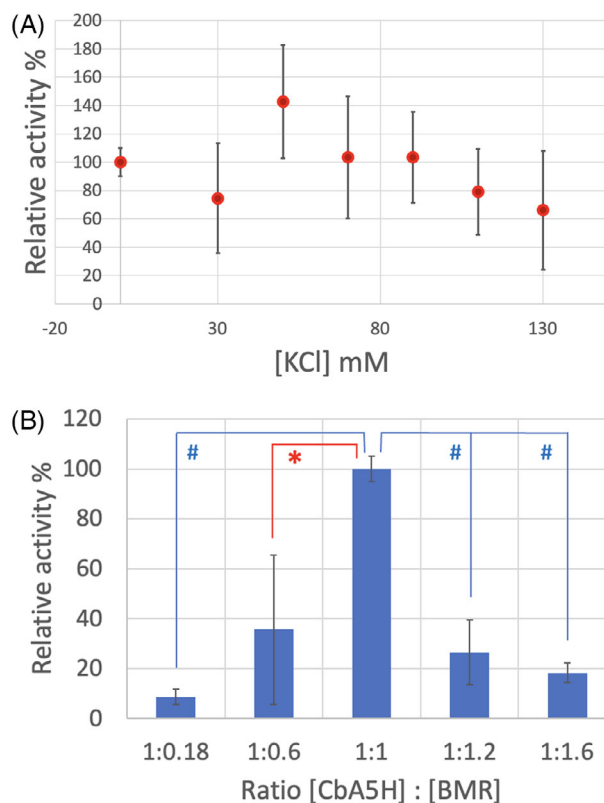
## 4 | DISCUSSION

The CbA5H hydrogenase from *C. beijerinckii* SM10[32] contains a novel domain called soluble ligand binding β-grasp or SLBB[58] whose structure was recently resolved as part of the N-terminal region of CbA5H[33] but whose role is still elusive. One possible function could be as an adapter region for interaction with alternative redox partners.
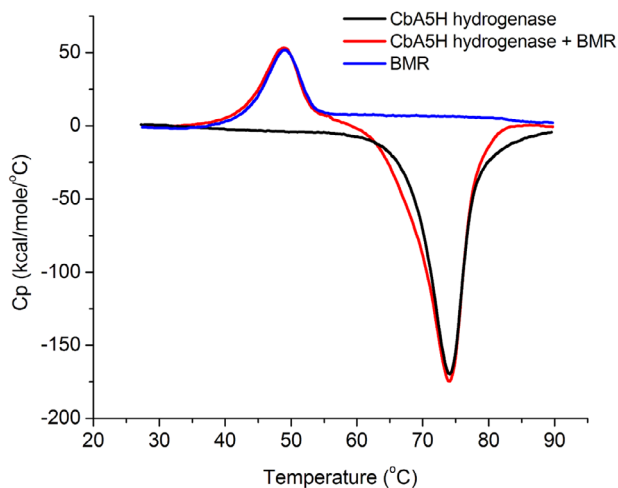
**FIGURE 4** Differential scanning calorimetry (DSC) scan trace for isolated BMR (blue) and CbA5H (black) and for the 1:1 mixture of both (red). The final concentration in the capillary was 8 µM for each of the tested protein, the test was performed in argon saturated buffer W, as described in Section 2.

This suggested to test this enzyme with non-physiological reductases, in order to achieve hydrogen sustained NAD(P)H reduction. Also, the general oxygen-resilience of this enzyme[30,32,33] makes it suitable for biotechnological applications.

The tests conducted for the regeneration of NAD(P)H are based on the use of CbA5H and two alternative reductases, physiologically involved in electron delivering to the heme of P450 enzymes, namely BMR, that is, the isolated reductase domain of the self-sufficient P450 BM3 from *B. megaterium* (now reclassified as *P. megaterium*) and human CPR.

The visual inspection of the structural and surface potential features of the involved redox partners (Figure 1) suggested a possible analogy of interaction of the strongly negative surface of the FMN binding domain of BMR or CPR (demonstrated to drive the interaction with physiological and non-physiological redox partners[59]) to positive regions of the CbA5H, which, in other hydrogenases (CaHydA or CpI), bind strongly negative ferredoxins as physiological redox partners.[60–62] It is to be noted that the FMN domain of BMR and CPR strongly resembles flavodoxin, a small flavoprotein which in evolution seems to have replaced ferredoxins as electron donor/acceptor[63] and which is still interchangeable with ferredoxin in certain systems.[64]

The activity tests in a hydrogen saturated solution clearly indicate that the hydrogen driven reaction of cofactor reduction can be accomplished in the CbA5H-BMR combination (Figures 2) both on NADP+ and NAD+, while CPR was never able to perform the reaction at a detectable level (Figure 2).

The reason for a specific preference of BMR could be ascribed to a better complementarity of BMR surface shape and charges with CbA5H than CPR, although the two reductases do not significantly differ and BMR can vicariate CPR in many reactions with human P450.[36,65]

A possible explanation of the very different behavior of BMR versus CPR as efficient electron exchanger to CbA5H is the different electron transfer process. In CPR two electrons from NADPH enter the enzyme to the FAD, followed by intramolecular electron transfer to FMN that shuttle between the semiquinone and hydroquinone states.[46,66] This also occurs in other CPRs from other mammalians[67] and from plants.[68] In the case of the bacterial system cytochrome P450 BM3, hence in BMR, the P450 heme is reduced by the anionic semiquinone of $FMNH^{\bullet-}$ rather than by $FMNH_2$, involving an equilibrium with the fully oxidized FMN in the FMN domain.[41,69] This could imply FMN of BMR is more prone to accept the one-electron transfer from the FeS cluster of CbA5H, transfer the electron from the anionic semiquinone of the $FMNH^{\bullet-}$ to the semiquinone $FADH^{\bullet}$, granting the reduced form able to transfer the two electrons pair to $NADP^+$. The equilibrium $FMNH_2$ (fully reduced hydroquinone) n $FMNH^{\bullet}$ (neutral semiquinone) in CPR would instead concentrate the electrons on the FMN domain, with possible backwards transfer to the hydrogenase moiety, more than toward the $FAD/NADP^+$ binding domain. The scheme reported in Figure 6 illustrates the proposed difference.

The optimal ratio CbA5H to BMR was found to be 1:1, suggesting a transient complex similar to the BMR complex to the isolated heme domain of P450-BM3 (BMP) or to other P450 heme subunit for which the BMR can vicariate the CPR.[36,65] The ITC measurements suggest a low endergonic energy of interaction, possibly due to conformational rearrangement in either of the two partners upon complex formation.

A lower concentration of BMR did not sustain the maximal activity. The increase in BMR concentration resulted in a decrease of the activity, hinting to a possible inhibitory effect, or a competing equilibrium. A dimerization was observed on the whole P450 BM3 of which BMR is a domain[70–73] but a direct BMR to BMR interaction was also observed under several conditions.[74,75] Here, a dimerization could compete with or hinder the productive interaction with CbA5H, leading to the strong decrease observed (Figure 3B).

The analysis of the single proteins involved and of the optimal 1:1 ratio combination of BMR and CbA5H performed by DSC confirmed a very good stability of the system (Figure 4). The BMR observed single peak is in line with previous reports[35,72,76] showing the endergonic denaturation process is not negatively affected by the presence of CbA5H, thus BMR is not destabilized. The CbA5H negative peak suggests an exergonic process which might be related to forming aggregates[77–78] or the result of the oxidation of strongly reducing compounds involved,[79] as here is the case for the Fe(I) and Fe(II) containing H-cluster of the hydrogenase, which might change solvent exposure and be oxidized upon denaturation of the protein scaffold.

In the 1:1 complex, in a low ionic strength buffer (suboptimal for the CbA5H activity) the increasing concentration of salt does not affect significantly the activity recorded (Figure 3A). The null effect of the ionic strength on the rate of NADPH production suggests that the surface-to-surface electrostatic interactions are not driving the complex stability in the productive form. This does not mean that an ionic strength effect must be completely excluded, more likely a mixed effect is in place together with the charge contribution, including other interactions (hydrophobic, dipole, van der Waals, etc.) shielding the simple salt effect.
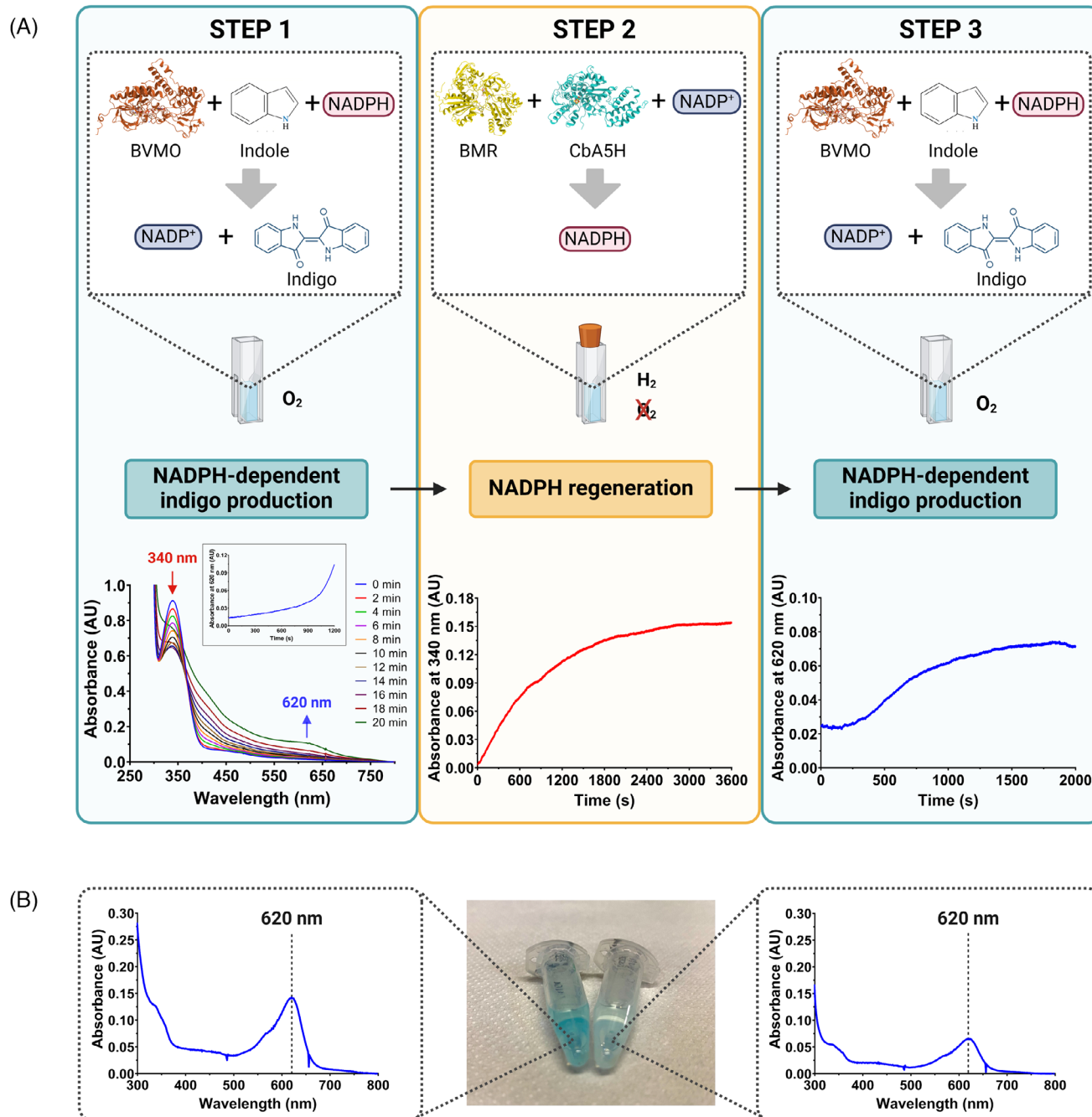
**FIGURE 5** Scheme and data on regeneration applied to indigo production mediated by Ar-BVMO R292A mutant. (A) STEP 1, aerobic indigo production, with the relevant protein involved (the system contains from the beginning 2 µM Ar-BVMO R292A mutant, 5 mM indole, 0.23 µM BMR, 0.23 µM CbA5H in buffer W and NADPH/NADP$^+$ from a previous round of NADPH production as described for Figure 2A). The spectra indicate the increase in absorbance at 620 nm due to accumulating indigo (inset reports the kinetic trace at 620 nm) following also NADPH consumption at 340 nm. At 20 min the recording already shows background increase due to precipitating indigo interference. STEP 2, anaerobic H$_2$ dependent NADPH regeneration in the supernatant after indigo-only centrifugation, with involved proteins and recorded trace at 340 nm of NADPH regeneration until plateau (corresponding spectra reported in Figure S4). STEP 3, aerobic use of regenerated NADPH in a second round of indigo production by Ar-BVMO R292A mutant, with kinetic trace of indigo accumulation, monitored at 620 nm. (B) Spectra of DMSO resuspended samples of produced indigo harvested after centrifugation of reactions in STEP 1 (left) and STEP 3 (right) with corresponding pictures of tubes containing the indigo solutions. Figure created with BioRender.com.
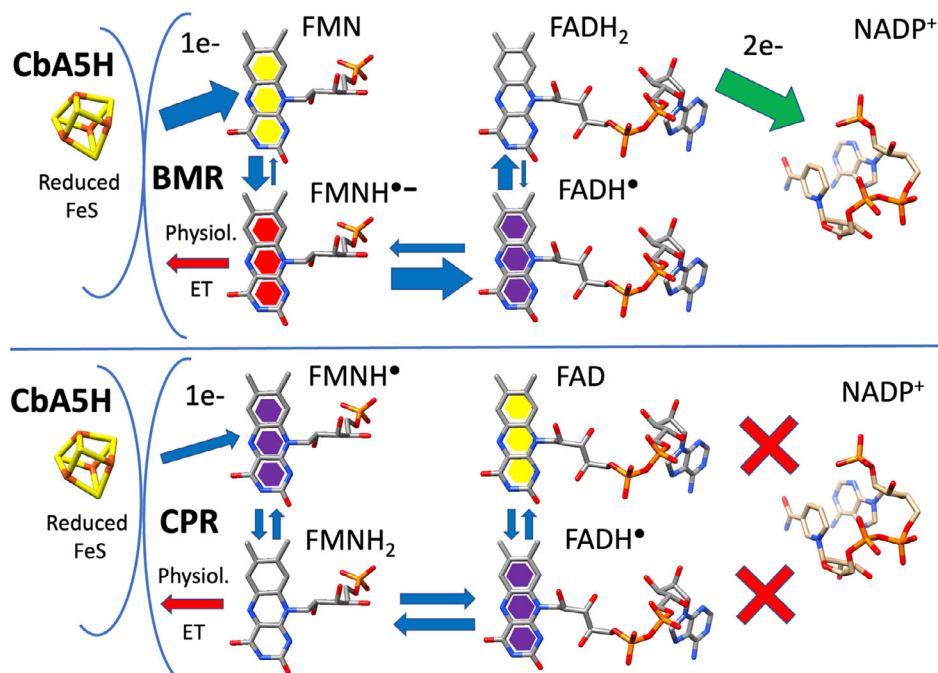
**FIGURE 6**    Scheme of the possible electron transfer (ET) pathway in the productive CbA5H-BMR complex versus the non-productive CbA5H-CPR complex. The red arrows indicate the physiological electron delivery reaction with the FMN reduced redox form transferring electrons as reported in the literature ($FMNH_2$ for CPR and $FMNH^{\bullet-}$ for BMR). The blue arrows indicate the 1 electron transfer reactions. FMN and FAD in the fully oxidized forms are highlighted in yellow, $FMNH^{\bullet}$ and $FADH^{\bullet}$ in the neutral semiquinone form are highlighted in violet, $FMNH^{\bullet-}$ in the anionic semiquinone in red, $FMNH_2$ and $FADH_2$ are not highlighted.

A value of $28 \pm 2$ nmol NADPH regenerated $s^{-1}$ mg of hydrogenase$^{-1}$ was calculated from the activity on NADP$^+$ (i.e., $1.68 \pm 0.12$ U mg$^{-1}$, TOF: $126 \pm 9$ min$^{-1}$), while values of $0.46 \pm 0.04$ nmol NADH regenerated $s^{-1}$ mg of hydrogenase $^{-1}$ (i.e., $0.028 \pm 0.002$ U mg$^{-1}$, TOF: $2.1 \pm 0.2$ min$^{-1}$) were recorded for the reduction of NAD$^+$. The lower reduction activities yielding NADH versus NADPH were expected, considering the BMR as the NAD(P)H recognizing scaffold. In fact, BMR was shown to be able to bind both NADPH and NADH, but with affinities which are higher for the phosphorylated form of the cofactor. The isolated BMR FAD and NAD(P)H binding domain was tested[80] and a $K_D$ of $23 \pm 6$ μM was reported for NADPH, while a $K_D$ of $10,900 \pm 1000$ μM was measured for NADH, showing a 470-fold lower affinity of NADH compared to NADPH. A similar ratio was reported[80] for the $K_M$ of NADPH versus NADH in the physiological reaction, that is, $6.5 \pm 1.3$ μM for NADPH and of $3030 \pm 730$ μM for NADH (about 500 folds higher). These data are coherent with a selective recognition of the phosphorylated form, confirmed by crystallography.[81] Also, a slow release of NADP$^+$ from the 2-electron-reduced enzyme was demonstrated in the wild-type FAD domain,[82] supporting a good affinity not only for the reduced form but also for the oxidized one, as tested here.

The TOF of FAD reduction in the isolated FAD and NAD(P)H binding domain of BMR are 18 times higher for NADPH.[80] In the system reported here the TOFs are 128 and 2.1 min$^{-1}$ for the whole reaction of NADP$^+$ and NAD$^+$ reduction, respectively, with a 60 times higher rates for NADP$^+$ over NAD$^+$ reduction. It is to be noted though, that, given a higher $K_M$ for NADH, a TOF of about 8.4 min$^{-1}$ could be reached at

higher concentrations for NAD$^+$ reduction, with a value about 15 times lower than NADP$^+$ reduction, consistent with the TOF ratio NADPH to NADH of 18 reported in the physiological reaction. Given the higher commercial value of NADPH over NADH, the selectivity here reported is already an advantage, but if necessary BMR can be redesigned to recognize NAD$^+$ over NADP$^+$.[73]

The NADP$^+$ reduction activity recorded ($1.68 \pm 0.12$ U mg$^{-1}$) is in line with other hydrogen-based NADPH regeneration systems, with a TOF reaching 50% of the best reported [NiFe]-hydrogenase SH from *C. necator* variant E341A/S342R (Table 1).

The soluble [NiFe]-hydrogenases (SH) from *P. furiosus* and *C. necator* were both used for NAD(P)H regeneration and are considered as a benchmark for this approach. The former can reach an activity of 1.55 U mg$^{-1}$ at 40°C,[24] having an intrinsic good affinity for the phosphorylated form of the cofactor, but the oxygen tolerance is quite low,[85] although it can be quickly reactivated. The SH from *C. necator* is oxygen tolerant and can work at oxygen concentration equivalent to aqueous solution equilibrated in air, but the WT enzyme had to be engineered to be able to recognize NADP$^+$, as the WT enzyme only regenerates NADH. The E341A/S342R variant reached an activity of $1.22 \pm 0.01$ U mg$^{-1}$ in absence of oxygen and of $1.15 \pm 0.02$ U mg$^{-1}$ in presence of 0.23 mM $O_2$. The CbA5H-BMR system cannot be active in oxygen, but alternated cycling of hydrogen, inert gas and oxygen could easily allow to regenerate NADPH and then use the cofactor to sustain the biotechnological reaction of interest. The system shows a good stability both in time and to repeated cycles of hydrogen re-flushing (Figure S2). Resilience of CbA5H to repeated oxygen exposure and full recovery

**TABLE 1** Comparison of enzymatic systems applied for hydrogen-driven NADPH regeneration.

| System | Activity NADPH [U mg$^{-1}$] | TOF [min$^{-1}$] | Oxygen tolerance (hydrogenase) | Reference |
|---|---|---|---|---|
| [FeFe]-hydrogenase CbA5H and BMR | $1.68 \pm 0.12$ | $126 \pm 9$ | CbA5H Resilient, i.e., inactive in oxygen but easily reactivated[32] | This work |
| [FeFe]-hydrogenase NADP-dependent (operon hndABCD) from *D. fructosovorans* | 0.013[a] | N.A. | Confirmed inactive protected state of Hnd but observed specificity for NAD$^+$[83] | [84] |
| [NiFe]-hydrogenase SH from *P. furiosus* WT | 1.55 | 0.73 (44 h$^{-1}$) | Partial tolerance to short (<200 s) exposure to 14 µM O$_2$, it can be reactivated[85] | [24] |
| [NiFe]-hydrogenase SH from *C. necator* variant E341A/S342R | $1.22 \pm 0.01$ ($-$O$_2$) $1.15 \pm 0.02$ ($+$O$_2$) | $360 \pm 2.4$ ($6.0 \pm 0.4$ s$^{-1}$) | Active in 0.23 mM O$_2$, equivalent to the O$_2$ level in aqueous solution equilibrated in air[52] | [52] |

[a]Value refers to soluble fraction from cell extract, no values available on purified enzyme on NADPH.

was already demonstrated[32] but further tests confirmed a very high mean residual activity after oxygen exposure (around 70%) in the system here proposed (Figure S3). A high variability of measurement and a slightly higher percentage of inactivation than previously observed (in some samples) might be due to the relatively low redox potential of the solution with accumulated NADPH, which could maintain a small amount of CbA5H in the unlocked and unprotected state, as previously suggested.[33]

Other systems based on [FeFe]-hydrogenase as the catalytic source of electron from H$_2$ have not, to the best of our knowledge, been able to regenerate NADPH. In fact, some [FeFe]-hydrogenases able to regenerate NADH were proposed, like the NADH-dependent, ferredoxin-independent [FeFe]-hydrogenase from *Syntrophomonas wolfei*.[86] The purified recombinant Hyd1ABC trimeric enzyme had high NAD$^+$-reducing activity with hydrogen as the electron donor (specific activity of 94.5 U mg$^{-1}$ at 37°C) but is not reported to be able to reduce NADP$^+$.

A putative NADP-reducing hydrogenase from *Desulfovibrio fructosovorans*[87,84] was reported to have activity in cytosolic cell lysates as indicated in Table 1.[84] This electron-bifurcating hydrogenase, called Hnd and encoded by the operon firstly reported as responsible for the NADP$^+$ reducing activity,[87,84] was recombinantly expressed in the tetrameric form,[83] but surprisingly it demonstrated a good NAD$^+$-reducing activity and no NADP$^+$ activity. In this work, the addition of the BMR module as redox partner of the [FeFe]-hydrogenase worked as an adapter for NAD(P)H interaction, granting to the system the ability to perform the regeneration, with a better performance on NADPH regeneration over NADH given the BMR specificity preferences.

As a proof-of-concept for exploitation in biocatalysis, the system was applied to regenerate NADPH for indigo production by Ar-BVMO R292A, showing that the regeneration cascade did not interfere with Ar-BVMO R292A catalysis and that multiple cycle of NADPH regeneration can be easily performed (Figure 5A, B).

In conclusion, this work demonstrated a novel concept of an artificial and stable two-component protein system able to sustain a good NADPH regeneration rate from hydrogen, with values comparable to [NiFe]-hydrogenases and the possibility to alternate cycles in hydrogen with reaction in presence of oxygen, given the reversible protected state of CbA5H. The novelty of using [FeFe]hydrogenase as catalyst, which is renowned to have much higher catalytic turnovers than [NiFe], holds a high potential as a valid alternative to consolidated methods. The system proposed here is the first of its kind, based on non-physiological partners simply used in solution. Important improvements can stem from protein engineering and creation of chimeric enzymes based on the modular combination called "Molecular Lego", which has already successfully employed BMR as a fused module to different enzymes.[35–40,88,89]

## AUTHOR CONTRIBUTIONS

## ACKNOWLEDGMENTS

## CONFLICT OF INTEREST STATEMENT

The authors declare that the research was conducted in the absence of any commercial or financial relationships that could be construed as a potential conflict of interest.

## DATA AVAILABILITY STATEMENT

The data that support the findings of this study are available from the corresponding author upon reasonable request.

## ORCID

*Lisa Barbieri* https://orcid.org/0009-0003-7975-5317
*Gianfranco Gilardi* https://orcid.org/0000-0002-6559-276X
*Francesca Valetti* https://orcid.org/0000-0002-8380-595X

## REFERENCES

1. Bell, E. L., Finnigan, W., France, S. P., Green, A. P., Hayes, M. A., Hepworth, L. J., Lovelock, S. L., Niikura, H., Osuna, S., Romero, E., Ryan, K. S., Turner, N. J., & Flitsch, S. L. (2021). Biocatalysis. *Nature Reviews Methods Primers*, *1*(1), 46. https://doi.org/10.1038/s43586-021-00044-z

2. Winkler, C. K., Schrittwieser, J. H., & Kroutil, W. (2021). Power of biocatalysis for organic synthesis. *ACS Central Science*, *7*(1), 55–71. https://doi.org/10.1021/acscentsci.0c01496

3. Intasian, P., Prakinee, K., Phintha, A., Trisrivirat, D., Weeranoppanant, N., Wongnate, T., & Chaiyen, P. (2021). Enzymes, *in vivo* biocatalysis, and metabolic engineering for enabling a circular economy and sustainability. *Chemical Reviews*, *121*(17), 10367–10451. https://doi.org/10.1021/acs.chemrev.1c00121

4. Wang, X., Saba, T., Yiu, H. H. P., Howe, R. F., Anderson, J. A., & Shi, J. (2017). Cofactor NAD(P)H regeneration inspired by heterogeneous pathways. *Chemistry*, *2*(5), 621–654. https://doi.org/10.1016/j.chempr.2017.04.009

5. Wu, H., Tian, C., Song, X., Liu, C., Yang, D., & Jiang, Z. (2013). Methods for the regeneration of nicotinamide coenzymes. *Green Chemistry*, *15*(7), 1773. https://doi.org/10.1039/c3gc37129h

6. Ma, S. K., Gruber, J., Davis, C., Newman, L., Gray, D., Wang, A., Grate, J., Huisman, G. W., & Sheldon, R. A. (2010). A green-by-design biocatalytic process for atorvastatin intermediate. *Green Chemistry*, *12*(1), 81–86. https://doi.org/10.1039/B919115C

7. Wichmann, R., Wandrey, C., Bückmann, A. F., & Kula, M. (1981). Continuous enzymatic transformation in an enzyme membrane reactor with simultaneous NAD(H) regeneration. *Biotechnology and Bioengineering*, *23*(12), 2789–2802. https://doi.org/10.1002/bit.260231213

8. Bommarius, A. S., Schwarm, M., Stingl, K., Kottenhahn, M., Huthmacher, K., & Drauz, K. (1995). Synthesis and use of enantiomerically pure tert-leucine. *Tetrahedron: Asymmetry*, *6*(12), 2851–2888. https://doi.org/10.1016/0957-4166(95)00377-0

9. Liu, W., Ma, H., Luo, J., Shen, W., Xu, X., Li, S., Hu, Y., & Huang, H. (2014). Efficient synthesis of l-tert-leucine through reductive amination using leucine dehydrogenase and formate dehydrogenase coexpressed in recombinant E. coli. *Biochemical Engineering Journal*, *91*, 204–209. https://doi.org/10.1016/j.bej.2014.08.003

10. Luo, W., Zhu, J., Zhao, Y., Zhang, H., Yang, X., Liu, Y., Rao, Z., & Yu, X. (2020). Cloning and expression of a novel leucine dehydrogenase: Characterization and L-tert-leucine production. *Frontiers in Bioengineering and Biotechnology*, *8*, 186. https://doi.org/10.3389/fbioe.2020.00186

11. Llinàs-Brunet, M., Bailey, M. D., Goudreau, N., Bhardwaj, P. K., Bordeleau, J., Bös, M., Bousquet, Y., Cordingley, M. G., Duan, J., Forgione, P., Garneau, M., Ghiro, E., Gorys, V., Goulet, S., Halmos, T., Kawai, S. H., Naud, J., Poupart, M.-A., & White, P. W. (2010). Discovery of a potent and selective noncovalent linear inhibitor of the hepatitis C virus NS3 protease (BI 201335). *Journal of Medicinal Chemistry*, *53*(17), 6466–6476. https://doi.org/10.1021/jm100690x

12. Qian, Z., Dougherty, P. G., Liu, T., Oottikkal, S., Hogan, P. G., Hadad, C. M., & Pei, D. (2014). Structure-based optimization of a peptidyl inhibitor against calcineurin-nuclear factor of activated T cell (NFAT) interaction. *Journal of Medicinal Chemistry*, *57*(18), 7792–7797. https://doi.org/10.1021/jm500743t

13. Guo, Q., Gakhar, L., Wickersham, K., Francis, K., Vardi-Kilshtain, A., Major, D. T., Cheatum, C. M., & Kohen, A. (2016). Structural and kinetic studies of formate dehydrogenase from *Candida boidinii*. *Biochemistry*, *55*(19), 2760–2771. https://doi.org/10.1021/acs.biochem.6b00181

14. Hu, D., Wen, Z., Li, C., Hu, B., Zhang, T., Li, J., & Wu, M. (2020). Characterization of a robust glucose 1-dehydrogenase, SyGDH, and its application in NADPH regeneration for the asymmetric reduction of haloketone by a carbonyl reductase in organic solvent/buffer system. *Process Biochemistry*, *89*, 55–62. https://doi.org/10.1016/j.procbio.2019.09.037

15. Lin, S., Sun, S., Wang, K., Shen, K., Ma, B., Ren, Y., & Fan, X. (2018). Bioinspired design of alcohol dehydrogenase@nano TiO2 microreactors for sustainable cycling of NAD+/NADH coenzyme. *Nanomaterials*, *8*(2), 127. https://doi.org/10.3390/nano8020127

16. Abdel-Hady, G. N., Ikeda, T., Ishida, T., Funabashi, H., Kuroda, A., & Hirota, R. (2021). Engineering cofactor specificity of a thermostable phosphite dehydrogenase for a highly efficient and robust NADPH regeneration system. *Frontiers in Bioengineering and Biotechnology*, *9*, 647176. https://doi.org/10.3389/fbioe.2021.647176

17. Johannes, T. W., Woodyer, R. D., & Zhao, H. (2007). Efficient regeneration of NADPH using an engineered phosphite dehydrogenase. *Biotechnology and Bioengineering*, *96*(1), 18–26. https://doi.org/10.1002/bit.21168

18. Oeggl, R., Neumann, T., Gätgens, J., Romano, D., Noack, S., & Rother, D. (2018). Citrate as cost-efficient NADPH regenerating agent. *Frontiers in Bioengineering and Biotechnology*, *6*, 196. https://doi.org/10.3389/fbioe.2018.00196

19. Arizzi, M., Morra, S., Pugliese, M., Gullino, M. L., Gilardi, G., & Valetti, F. (2016). Biohydrogen and biomethane production sustained by untreated matrices and alternative application of compost waste. *Waste Management (New York, N.Y.)*, *56*, 151–157. https://doi.org/10.1016/j.wasman.2016.06.039

20. Lopez-Hidalgo, A. M., Smoliński, A., & Sanchez, A. (2022). A meta-analysis of research trends on hydrogen production via dark fermentation. *International Journal of Hydrogen Energy*, *47*(27), 13300–13339. https://doi.org/10.1016/j.ijhydene.2022.02.106

21. Yue, M., Lambert, H., Pahon, E., Roche, R., Jemei, S., & Hissel, D. (2021). Hydrogen energy systems: A critical review of technologies, applications, trends and challenges. *Renewable & Sustainable Energy Reviews*, *146*, 111180. https://doi.org/10.1016/j.rser.2021.111180

22. Kayfeci, M., Keçebaş, A., & Bayat, M. (2019). Hydrogen production. In *Solar hydrogen production* (pp. 45–83). Elsevier. https://doi.org/10.1016/B978-0-12-814853-2.00003-5

23. Greiner, L., Schröder, I., Müller, D. H., & Liese, A. (2003). Utilization of adsorption effects for the continuous reduction of NADP +

with molecular hydrogen by Pyrococcus furiosus hydrogenase. *Green Chemistry*, 5(6), 697–700. https://doi.org/10.1039/B306915J

24. Mertens, R., Greiner, L., Van Den Ban, E. C. D., Haaker, H. B. C. M., & Liese, A. (2003). Practical applications of hydrogenase I from Pyrococcus furiosus for NADPH generation and regeneration. *Journal of Molecular Catalysis B: Enzymatic*, 24–25, 39–52. https://doi.org/10.1016/S1381-1177(03)00071-7

25. Wu, C.-H., McTernan, P. M., Walter, M. E., & Adams, M. W. W. (2015). Production and application of a soluble hydrogenase from *Pyrococcus furiosus*. *Archaea*, 2015, 1–8. https://doi.org/10.1155/2015/912582

26. Burgdorf, T., Van Der Linden, E., Bernhard, M., Yin, Q. Y., Back, J. W., Hartog, A. F., Muijsers, A. O., De Koster, C. G., Albracht, S. P. J., & Friedrich, B. (2005). The soluble NAD$^+$-reducing [NiFe]-hydrogenase from *Ralstonia eutropha* H16 consists of six subunits and can be specifically activated by NADPH. *Journal of Bacteriology*, 187(9), 3122–3132. https://doi.org/10.1128/JB.187.9.3122-3132.2005

27. Ratzka, J., Lauterbach, L., Lenz, O., & Ansorge-Schumacher, M. B. (2011). Systematic evaluation of the dihydrogen-oxidising and NAD$^+$-reducing soluble [NiFe]-hydrogenase from Ralstonia eutropha H16 as a cofactor regeneration catalyst. *Biocatalysis and Biotransformation*, 29(6), 246–252. https://doi.org/10.3109/10242422.2011.615393

28. Lubitz, W., Ogata, H., Rüdiger, O., & Reijerse, E. (2014). Hydrogenases. *Chemical Reviews*, 114(8), 4081–4148. https://doi.org/10.1021/cr4005814

29. Morra, S. (2022). Fantastic [FeFe]-hydrogenases and where to find them. *Frontiers in Microbiology*, 13, 853626. https://doi.org/10.3389/fmicb.2022.853626

30. Corrigan, P. S., Tirsch, J. L., & Silakov, A. (2020). Investigation of the unusual ability of the [FeFe] hydrogenase from Clostridium beijerinckii to access an O2-protected state. *Journal of the American Chemical Society*, 142(28), 12409–12419. https://doi.org/10.1021/jacs.0c04964

31. Heghmanns, M., Rutz, A., Kutin, Y., Engelbrecht, V., Winkler, M., Happe, T., & Kasanmascheff, M. (2022). The oxygen-resistant [FeFe]-hydrogenase CbA5H harbors an unknown radical signal. *Chemical Science*, 13(24), 7289–7294. https://doi.org/10.1039/D2SC00385F

32. Morra, S., Arizzi, M., Valetti, F., & Gilardi, G. (2016). Oxygen stability in the new [FeFe]-hydrogenase from *Clostridium beijerinckii* SM10 (CbA5H). *Biochemistry*, 55(42), 5897–5900. https://doi.org/10.1021/acs.biochem.6b00780

33. Winkler, M., Duan, J., Rutz, A., Felbek, C., Scholtysek, L., Lampret, O., Jaenecke, J., Apfel, U.-P., Gilardi, G., Valetti, F., Fourmond, V., Hofmann, E., Léger, C., & Happe, T. (2021). A safety cap protects hydrogenase from oxygen attack. *Nature Communications*, 12(1), 756. https://doi.org/10.1038/s41467-020-20861-2

34. Rutz, A., Das, C. K., Fasano, A., Jaenecke, J., Yadav, S., Apfel, U.-P., Engelbrecht, V., Fourmond, V., Léger, C., Schäfer, L. V., & Happe, T. (2023). Increasing the O$_2$ resistance of the [FeFe]-hydrogenase CbA5H through enhanced protein flexibility. *ACS Catalysis*, 13(2), 856–865. https://doi.org/10.1021/acscatal.2c04031

35. Catucci, G., Ciaramella, A., Di Nardo, G., Zhang, C., Castrignanò, S., & Gilardi, G. (2022). Molecular lego of human cytochrome P450: The key role of heme domain flexibility for the activity of the chimeric proteins. *International Journal of Molecular Sciences*, 23(7), 3618. https://doi.org/10.3390/ijms23073618

36. Dodhia, V. R., Fantuzzi, A., & Gilardi, G. (2006). Engineering human cytochrome P450 enzymes into catalytically self-sufficient chimeras using molecular Lego. *JBIC Journal of Biological Inorganic Chemistry*, 11(7), 903–916. https://doi.org/10.1007/s00775-006-0144-3

37. Giuriato, D., Correddu, D., Catucci, G., Di Nardo, G., Bolchi, C., Pallavicini, M., & Gilardi, G. (2022). Design of a H$_2$O$_2$-generating P450 SP$\alpha$ fusion protein for high yield fatty acid conversion. *Protein Science*, 31(12), e4501. https://doi.org/10.1002/pro.4501

38. McLean, K. J., Girvan, H. M., & Munro, A. W. (2007). Cytochrome P450/redox partner fusion enzymes: Biotechnological and toxicolog-

ical prospects. *Expert Opinion on Drug Metabolism & Toxicology*, 3(6), 847–863. https://doi.org/10.1517/17425255.3.6.847

39. Sadeghi, S. J., Meharenna, Y. T., Fantuzzi, A., Valetti, F., & Gilardi, G. (2000). Engineering artificial redox chains by molecular 'Lego'. *Faraday Discussions*, 116, 135–153. https://doi.org/10.1039/b003180l

40. Sadeghi, S. J., & Gilardi, G. (2013). Chimeric P 450 enzymes: Activity of artificial redox fusions driven by different reductases for biotechnological applications. *Biotechnology and Applied Biochemistry*, 60(1), 102–110. https://doi.org/10.1002/bab.1086

41. Sevrioukova, I., Shaffer, C., Ballou, D. P., & Peterson, J. A. (1996). Equilibrium and transient state spectrophotometric studies of the mechanism of reduction of the flavoprotein domain of P450BM-3. *Biochemistry*, 35(22), 7058–7068. https://doi.org/10.1021/bi960060a

42. Yun, C. H., Kim, K. H., Kim, D. H., Jung, H. C., & Pan, J. G. (2007). The bacterial P450 BM3: A prototype for a biocatalyst with human P450 activities. *Trends in Biotechnology*, 25(7), 289–298. https://doi.org/10.1016/j.tibtech.2007.05.003

43. Laursen, T., Jensen, K., & Møller, B. L. (2011). Conformational changes of the NADPH-dependent cytochrome P450 reductase in the course of electron transfer to cytochromes P450. *Biochimica et Biophysica Acta (BBA)—Proteins and Proteomics*, 1814(1), 132–138. https://doi.org/10.1016/j.bbapap.2010.07.003

44. Di Nardo, G., & Gilardi, G. (2020). Natural compounds as pharmaceuticals: The key role of cytochromes P450 reactivity. *Trends in Biochemical Sciences*, 45(6), 511–525. https://doi.org/10.1016/j.tibs.2020.03.004

45. Guengerich, F. P., & Munro, A. W. (2013). Unusual cytochrome P450 enzymes and reactions. *Journal of Biological Chemistry*, 288(24), 17065–17073. https://doi.org/10.1074/jbc.R113.462275

46. Ortiz De Montellano, P. R. (Ed.). (2015). *Cytochrome P450: Structure, mechanism, and biochemistry*. Springer International Publishing. https://doi.org/10.1007/978-3-319-12108-6

47. Wang, M., Roberts, D. L., Paschke, R., Shea, T. M., Masters, B. S. S., & Kim, J. J. P. (1997). Three-dimensional structure of NADPH–cytochrome P450 reductase: Prototype for FMN- and FAD-containing enzymes. *Proceedings of the National Academy of Sciences U S A*, 94(16), 8411–8416. https://doi.org/10.1073/pnas.94.16.8411

48. King, P. W., Posewitz, M. C., Ghirardi, M. L., & Seibert, M. (2006). Functional studies of [FeFe] hydrogenase maturation in an *Escherichia coli* biosynthetic system. *Journal of Bacteriology*, 188(6), 2163–2172. https://doi.org/10.1128/JB.188.6.2163-2172.2006

49. Morra, S., Cordara, A., Gilardi, G., & Valetti, F. (2015). Atypical effect of temperature tuning on the insertion of the catalytic iron—sulfur center in a recombinant [FeFe]-hydrogenase. *Protein Science*, 24(12), 2090–2094. https://doi.org/10.1002/pro.2805

50. Zhang, C., Catucci, G., Di Nardo, G., & Gilardi, G. (2020). Effector role of cytochrome P450 reductase for androstenedione binding to human aromatase. *International Journal of Biological Macromolecules*, 164, 510–517. https://doi.org/10.1016/j.ijbiomac.2020.07.163

51. Porter, T. D., Wilson, T. E., & Kasper, C. B. (1987). Expression of a functional 78,000 dalton mammalian flavoprotein, NADPH-cytochrome P-450 oxidoreductase, in Escherichia coli. *Archives of Biochemistry and Biophysics*, 254(1), 353–367. https://doi.org/10.1016/0003-9861(87)90111-1

52. Preissler, J., Reeve, H. A., Zhu, T., Nicholson, J., Urata, K., Lauterbach, L., Wong, L. L., Vincent, K. A., & Lenz, O. (2020). Dihydrogen-driven NADPH recycling in imine reduction and P450-catalyzed oxidations mediated by an engineered O 2-tolerant hydrogenase. *ChemCatChem*, 12(19), 4853–4861. https://doi.org/10.1002/cctc.202000763

53. Lauterbach, L., Idris, Z., Vincent, K. A., & Lenz, O. (2011). Catalytic properties of the isolated diaphorase fragment of the NAD+-reducing [NiFe]-hydrogenase from Ralstonia eutropha. *PLoS ONE*, 6(10), e25939. https://doi.org/10.1371/journal.pone.0025939

54. Gao, C., Catucci, G., Castrignanò, S., Gilardi, G., & Sadeghi, S. J. (2017). Inactivation mechanism of N61S mutant of human FMO3

towards trimethylamine. *Scientific Reports*, *7*(1), 14668. https://doi.org/10.1038/s41598-017-15224-9

55. Catucci, G., Aramini, D., Sadeghi, S. J., & Gilardi, G. (2020). Ligand stabilization and effect on unfolding by polymorphism in human flavin-containing monooxygenase 3. *International Journal of Biological Macromolecules*, *162*, 1484–1493. https://doi.org/10.1016/j.ijbiomac.2020.08.032

56. Catucci, G., Zgrablic, I., Lanciani, F., Valetti, F., Minerdi, D., Ballou, D. P., Gilardi, G., & Sadeghi, S. J. (2016). Characterization of a new Baeyer-Villiger monooxygenase and conversion to a solely N-or S-oxidizing enzyme by a single R292 mutation. *Biochimica et Biophysica Acta*, *1864*(9), 1177–1187. https://doi.org/10.1016/j.bbapap.2016.06.010

57. Catucci, G., Turella, S., Cheropkina, H., De Angelis, M., Gilardi, G., & Sadeghi, S. J. (2022). Green production of indigo and indirubin by an engineered Baeyer–Villiger monooxygenase. *Biocatalysis and Agricultural Biotechnology*, *44*, 102458. https://doi.org/10.1016/j.bcab.2022.102458

58. Burroughs, A. M., Balaji, S., Iyer, L. M., & Aravind, L. (2007). A novel superfamily containing the $\beta$-grasp fold involved in binding diverse soluble ligands. *Biology Direct*, *2*(1), 4. https://doi.org/10.1186/1745-6150-2-4

59. Davydov, D. R., Kariakin, A. A., Petushkova, N. A., & Peterson, J. A. (2000). Association of cytochromes P450 with their reductases: Opposite sign of the electrostatic interactions in P450BM-3 as compared with the microsomal 2B4 system. *Biochemistry*, *39*(21), 6489–6497. https://doi.org/10.1021/bi992936u

60. Brown, K. A., Wilker, M. B., Boehm, M., Dukovic, G., & King, P. W. (2012). Characterization of photochemical processes for H 2 production by CdS nanorod–[FeFe] hydrogenase complexes. *Journal of the American Chemical Society*, *134*(12), 5627–5636. https://doi.org/10.1021/ja2116348

61. Artz, J. H., Mulder, D. W., Ratzloff, M. W., Lubner, C. E., Zadvornyy, O. A., LeVan, A. X., Williams, S. G., Adams, M. W. W., Jones, A. K., King, P. W., & Peters, J. W. (2017). Reduction potentials of [FeFe]-hydrogenase accessory iron–sulfur clusters provide insights into the energetics of proton reduction catalysis. *Journal of the American Chemical Society*, *139*(28), 9544–9550. https://doi.org/10.1021/jacs.7b02099

62. Gauquelin, C., Baffert, C., Richaud, P., Kamionka, E., Etienne, E., Guieysse, D., Girbal, L., Fourmond, V., André, I., Guigliarelli, B., Léger, C., Soucaille, P., & Meynial-Salles, I. (2018). Roles of the F-domain in [FeFe] hydrogenase. *Biochimica et Biophysica Acta (BBA)—Bioenergetics*, *1859*(2), 69–77. https://doi.org/10.1016/j.bbabio.2017.08.010

63. Campbell, I. J., Bennett, G. N., & Silberg, J. J. (2019). Evolutionary relationships between low potential ferredoxin and flavodoxin electron carriers. Frontiers in Energy Research, *7*, 79. https://doi.org/10.3389/fenrg.2019.00079

64. Poudel, S., Colman, D. R., Fixen, K. R., Ledbetter, R. N., Zheng, Y., Pence, N., Seefeldt, L. C., Peters, J. W., Harwood, C. S., & Boyd, E. S. (2018). Electron transfer to nitrogenase in different genomic and metabolic backgrounds. *Journal of Bacteriology*, *200*(10). https://doi.org/10.1128/JB.00757-17

65. Degregorio, D., D'Avino, S., Castrignanò, S., Di Nardo, G., Sadeghi, S. J., Catucci, G., & Gilardi, G. (2017). Human cytochrome P450 3A4 as a biocatalyst: Effects of the engineered linker in modulation of coupling efficiency in 3A4-BMR chimeras. Frontiers in Pharmacology, *8*, 121. https://doi.org/10.3389/fphar.2017.00121

66. Iyanagi, T., Xia, C., & Kim, J.-J. P. (2012). NADPH–cytochrome P450 oxidoreductase: Prototypic member of the diflavin reductase family. *Archives of Biochemistry and Biophysics*, *528*(1), 72–89. https://doi.org/10.1016/j.abb.2012.09.002

67. Iyanagi, T., Makino, N., & Mason, H. S. (1974). Redox properties of the reduced nicotinamide adenine dinucleotide phosphate-cytochrome P-450 and reduced nicotinamide adenine dinucleotide-cytochrome b5 reductases. *Biochemistry*, *13*(8), 1701–1710. https://doi.org/10.1021/bi00705a023

68. Zhang, B., Kang, C., & Davydov, D. R. (2022). Conformational rearrangements in the redox cycling of NADPH-cytochrome P450 reductase from Sorghum bicolor explored with FRET and pressure-perturbation spectroscopy. *Biology*, *11*(4), 510. https://doi.org/10.3390/biology11040510

69. Sevrioukova, I. F., & Peterson, J. A. (1995). NADPH-P-450 reductase: Structural and functional comparisons of the eukaryotic and prokaryotic isoforms. *Biochimie*, *77*(7), 562–572. https://doi.org/10.1016/0300-9084(96)88172-7

70. Black, S. D., & Martin, S. T. (1994). Evidence for conformational dynamics and molecular aggregation in cytochrome P450 102 (BM-3). *Biochemistry*, *33*(40), 12056–12062. https://doi.org/10.1021/bi00206a007

71. Jamakhandi, A. P., Jeffus, B. C., Dass, V. R., & Miller, G. P. (2005). Thermal inactivation of the reductase domain of cytochrome P450 BM3. *Archives of Biochemistry and Biophysics*, *439*(2), 165–174. https://doi.org/10.1016/j.abb.2005.04.022

72. Neeli, R., Girvan, H. M., Lawrence, A., Warren, M. J., Leys, D., Scrutton, N. S., & Munro, A. W. (2005). The dimeric form of flavocytochrome P450 BM3 is catalytically functional as a fatty acid hydroxylase. *FEBS Letters*, *579*(25), 5582–5588. https://doi.org/10.1016/j.febslet.2005.09.023

73. Girvan, H. M., Dunford, A. J., Neeli, R., Ekanem, I. S., Waltham, T. N., Joyce, M. G., Leys, D., Curtis, R. A., Williams, P., Fisher, K., Voice, M. W., & Munro, A. W. (2011). Flavocytochrome P450 BM3 mutant W1046A is a NADH-dependent fatty acid hydroxylase: Implications for the mechanism of electron transfer in the P450 BM3 dimer. *Archives of Biochemistry and Biophysics*, *507*(1), 75–85. https://doi.org/10.1016/j.abb.2010.09.014

74. Zhang, H., Yokom, A. L., Cheng, S., Su, M., Hollenberg, P. F., Southworth, D. R., & Osawa, Y. (2018). The full-length cytochrome P450 enzyme CYP102A1 dimerizes at its reductase domains and has flexible heme domains for efficient catalysis. *Journal of Biological Chemistry*, *293*(20), 7727–7736. https://doi.org/10.1074/jbc.RA117.000600

75. Jeffreys, L. N., Pacholarz, K. J., Johannissen, L. O., Girvan, H. M., Barran, P. E., Voice, M. W., & Munro, A. W. (2020). Characterization of the structure and interactions of P450 BM3 using hybrid mass spectrometry approaches. *Journal of Biological Chemistry*, *295*(22), 7595–7607. https://doi.org/10.1074/jbc.RA119.011630

76. Butler, C. F., Peet, C., Mason, A. E., Voice, M. W., Leys, D., & Munro, A. W. (2013). Key mutations alter the cytochrome P450 BM3 conformational landscape and remove inherent substrate bias. *Journal of Biological Chemistry*, *288*(35), 25387–25399. https://doi.org/10.1074/jbc.M113.479717

77. Fitzsimons, S. M., Mulvihill, D. M., & Morris, E. R. (2007). Denaturation and aggregation processes in thermal gelation of whey proteins resolved by differential scanning calorimetry. *Food Hydrocolloids*, *21*(4), 638–644. https://doi.org/10.1016/j.foodhyd.2006.07.007

78. Goyal, M., Chaudhuri, T. K., & Kuwajima, K. (2014). Irreversible denaturation of maltodextrin glucosidase studied by differential scanning calorimetry, circular dichroism, and turbidity measurements. *PLoS ONE*, *9*(12), e115877. https://doi.org/10.1371/journal.pone.0115877

79. Gill, P., Moghadam, T. T., & Ranjbar, B. (2010). Differential scanning calorimetry techniques: Applications in biology and nanoscience. *Journal of Biomolecular Techniques : JBT*, *21*(4), 167–193.

80. Dunford, A. J., Girvan, H. M., Scrutton, N. S., & Munro, A. W. (2009). Probing the molecular determinants of coenzyme selectivity in the P450 BM3 FAD/NADPH domain. *Biochimica et Biophysica Acta (BBA)—Proteins and Proteomics*, *1794*(8), 1181–1189. https://doi.org/10.1016/j.bbapap.2009.03.014

81. Joyce, M. G., Ekanem, I. S., Roitel, O., Dunford, A. J., Neeli, R., Girvan, H. M., Baker, G. J., Curtis, R. A., Munro, A. W., & Leys, D. (2012). The crystal structure of the FAD/NADPH-binding domain of flavocy-

tochrome P450 BM3. *FEBS Journal*, 279(9), 1694–1706. https://doi.org/10.1111/j.1742-4658.2012.08544.x

82. Roitel, O., Scrutton, N. S., & Munro, A. W. (2003). Electron transfer in flavocytochrome P450 BM3: Kinetics of flavin reduction and oxidation, the role of cysteine 999, and relationships with mammalian cytochrome P450 reductase. *Biochemistry*, 42(36), 10809–10821. https://doi.org/10.1021/bi034562h

83. Kpebe, A., Benvenuti, M., Guendon, C., Rebai, A., Fernandez, V., Le Laz, S., Etienne, E., Guigliarelli, B., García-Molina, G., De Lacey, A. L., Baffert, C., & Brugna, M. (2018). A new mechanistic model for an O2-protected electron-bifurcating hydrogenase, Hnd from Desulfovibrio fructosovorans. *Biochimica et Biophysica Acta (BBA)−Bioenergetics*, 1859(12), 1302–1312. https://doi.org/10.1016/j.bbabio.2018.09.364

84. De Luca, G., De Philip, P., Rousset, M., Belaich, J. P., & Dermoun, Z. (1998). The NADP-reducing hydrogenase of Desulfovibrio fructosovorans: Evidence for a native complex with hydrogen-dependent methyl-viologen-reducing activity. *Biochemical and Biophysical Research Communications*, 248(3), 591–596. https://doi.org/10.1006/bbrc.1998.9022

85. Kwan, P., McIntosh, C. L., Jennings, D. P., Hopkins, R. C., Chandrayan, S. K., Wu, C.-H., Adams, M. W. W., & Jones, A. K. (2015). The [NiFe]-hydrogenase of *Pyrococcus furiosus* exhibits a new type of oxygen tolerance. *Journal of the American Chemical Society*, 137(42), 13556–13565. https://doi.org/10.1021/jacs.5b07680

86. Losey, N. A., Mus, F., Peters, J. W., Le, H. M., & McInerney, M. J. (2017). Syntrophomonas wolfei uses an NADH-dependent, ferredoxin-independent [FeFe]-hydrogenase to reoxidize NADH. *Applied and Environmental Microbiology*, 83(20), e01335–e01317. https://doi.org/10.1128/AEM.01335-17

87. Malki, S., Saimmaime, I., De Luca, G., Rousset, M., Dermoun, Z., & Belaich, J. P. (1995). Characterization of an operon encoding an NADP-reducing hydrogenase in Desulfovibrio fructosovorans. *Journal of Bacteriology*, 177(10), 2628–2636. https://doi.org/10.1128/jb.177.10.2628-2636.1995

88. Kokorin, A., Parshin, P. D., Bakkes, P. J., Pometun, A. A., Tishkov, V. I., & Urlacher, V. B. (2021). Genetic fusion of P450 BM3 and formate dehydrogenase towards self-sufficient biocatalysts with enhanced activity. *Scientific Reports*, 11(1), 21706. https://doi.org/10.1038/s41598-021-00957-5

89. Jetzschmann, K. J., Yarman, A., Rustam, L., Kielb, P., Urlacher, V. B., Fischer, A., Weidinger, I. M., Wollenberger, U., & Scheller, F. W. (2018). Molecular LEGO by domain-imprinting of cytochrome P450 BM3. *Colloids and Surfaces B: Biointerfaces*, 164, 240–246. https://doi.org/10.1016/j.colsurfb.2018.01.047

## SUPPORTING INFORMATION

Additional supporting information can be found online in the Supporting Information section at the end of this article.